

## Variability of $\eta$ Carinae

P. A. Whitelock,<sup>1</sup> M. W. Feast,<sup>2</sup> C. Koen,<sup>1</sup> G. Roberts<sup>1</sup> and B. S. Carter<sup>1</sup>

<sup>1</sup>South African Astronomical Observatory, PO Box 9, 7935 Observatory, South Africa

<sup>2</sup>Astronomy Department, University of Cape Town, Private Bag, 7700 Rondebosch, South Africa

Accepted 1994 April 25. Received 1994 April 11; in original form 1994 January 24

### ABSTRACT

Infrared (1.25–3.5  $\mu\text{m}$ ) light curves of  $\eta$  Carinae covering the last 20 yr are presented and discussed. Three features are clearly seen in these data. First there is an apparently secular increase in the brightness at the shorter wavelengths (1.25–2  $\mu\text{m}$ ), which is also seen in optical data. If this is due to the gradual thinning of dust in the homunculus, then this dust must be predominantly in the form of large grains. Secondly, quasi-periodic variations on a time-scale of about 5 yr are evident. These may be related to the moderate-amplitude variations observed in luminous blue variables. Thirdly, there is evidence for changes on a time-scale of less than 100 d, which are also seen in independent optical photometry. Two possible mechanisms are considered for the quasi-periodic changes: deterministic pulsations and noise-driven pseudo-cyclicity.

**Key words:** stars: individual:  $\eta$  Carinae – stars: variable: other – dust, extinction – ISM: jets and outflows – infrared: stars.

### 1 INTRODUCTION

There is still controversy concerning the nature and evolutionary status of  $\eta$  Carinae, although it is usually assumed to have had a very massive progenitor and to be an extreme member of the class of luminous blue variables (LBVs). The LBVs are thought to represent an evolutionary phase between blue supergiants and Wolf-Rayets for stars with very massive ( $M_i \gtrsim 50 M_\odot$ ) progenitors (e.g. Maeder 1990). However, the structure of the homunculus nebula which surrounds  $\eta$  Carinae, and the existence of a stellar jet, revealed by *HST* observations (Hester et al. 1991), might be most easily explained as the products of an interacting binary (e.g. Bath 1979; Gallagher 1989). More exotic models have also been proposed (e.g. Borgwald & Friedlander 1993).

$\eta$  Carinae has a long history of optical variability (cf. Innes 1903; de Vaucouleurs & Eggen 1952; O'Connell 1956; Gratton 1963; Feinstein & Marraco 1974). The few estimates prior to 1800 indicate that it was brighter than at present, and variable. It reached maximum optical brightness,  $m_v \sim -1$  mag, in 1843. This was followed by a decline, which left it at  $m_v \sim 8$  mag for much of the first half of the 20th century. Since the discovery that  $\eta$  Carinae is very luminous in the infrared (Neugebauer & Westphal 1968; Westphal & Neugebauer 1969), it has been generally assumed that the major decline after 1843 followed the condensation of dust in the ejecta. The dust absorbs

radiation from the central source and re-emits it in the infrared. The more recent variability of  $\eta$  Carinae has been discussed by Whitelock et al. (1983, hereafter Paper I), van Genderen & Thé (1984), Zanella, Wolf & Stahl (1984) and van Genderen, de Groot & Thé (1994).

Very massive stars are predicted to be unstable to pulsation and to experience heavy mass loss (e.g. Appenzeller 1986; de Koter 1993). However, the details are obscure, and it is therefore of considerable interest to monitor such stars for periodic and secular variability. For  $\eta$  Carinae, a study of the variability also offers a potential method for discriminating between various models. Unfortunately, the extended nature of  $\eta$  Carinae makes it a particularly difficult source to monitor. As discussed below, the visual light is dominated by scattering from the  $\sim 12 \times 17$  arcsec<sup>2</sup> homunculus nebula. At wavelengths longer than 10  $\mu\text{m}$ , the radiation originates from cool ( $\lesssim 400\text{-K}$ ) dust in the homunculus, and the image is therefore extended, with a diameter of about 10 arcsec at 10  $\mu\text{m}$  (Hyland et al. 1979). The image diameter reaches a minimum of  $\sim 2$  arcsec near 2.2  $\mu\text{m}$  (Allen 1989). Although the emission at this wavelength arises from more than one component, it is dominated by dust close to the central source which is hotter than the bulk of material in the homunculus (Paper I). 2  $\mu\text{m}$  or thereabouts is therefore a particularly useful wavelength region at which to monitor  $\eta$  Carinae for changes in the central source.

## 2 THE PHOTOMETRY

A near-infrared (*JHKL*) monitoring programme for  $\eta$  Carinae has been in progress at the SAAO since 1972. Table 1 lists infrared photometry made on 156 nights between 1975 and 1994. The first column gives the Julian Date (JD)

of each observation. It includes 59 observations obtained prior to 1983 and discussed in Paper I, which have since been revised using Carter's (1990) values for the standard stars. The revisions are slight and do not affect the conclusions of Paper I. The recent data were obtained with the SAAO Mk II photometer on the 0.75-m reflector at

**Table 1.** Near-infrared photometry of  $\eta$  Carinae.

JD -2440000	J	H	K	L	JD -2440000	J	H	K	L	JD -2440000	J	H	K	L
	(mag)					(mag)					(mag)			
2491.	3.33	2.56	1.05	-1.66	4950.58	3.12	2.11	0.78	-1.69	6784.57	3.11	2.04	0.77	-1.58
2830.	3.29	2.24			4956.58	3.05	2.06	0.71	-1.77	6803.59	3.08	2.01	0.72	-1.65
3136.	3.11	2.36	0.98	-1.67	4958.57	3.08	2.07	0.73	-1.67	6825.45	3.08	2.00	0.71	-1.65
3173.51	3.16	2.40	1.02	-1.66	5006.51	3.11	2.12	0.79	-1.75	6831.49	3.06	1.99	0.69	-1.68
3197.48	3.24			-1.64	5017.48	3.11	2.11	0.77	-1.71	6844.49	3.09	2.03	0.70	-1.64
3222.42	3.18	2.42	1.04	-1.64	5022.41	3.11	2.12	0.80	-1.72	6848.46	3.10	2.02	0.69	-1.67
3235.39	3.11	2.41	1.03	-1.59	5033.52	3.13	2.12	0.80	-1.63	6873.41	3.12	2.07	0.74	-1.65
3251.32	3.18	2.40	1.02	-1.59	5060.37	3.12	2.12	0.78	-1.68	6894.36	3.11	2.09	0.75	-1.70
3251.32	3.17	2.39	1.02	-1.58	5094.29	3.11	2.13	0.79	-1.69	6924.30	3.17	2.11	0.78	-1.62
3521.56	3.41	2.45	1.03	-1.62	5119.21	3.14	2.15	0.82	-1.61	6959.32	3.15	2.11	0.76	-1.65
3554.55	3.43	2.48	1.06	-1.57	5121.21	3.13	2.14	0.80	-1.66	6984.22	3.18	2.12	0.78	-1.63
3554.55	3.43	2.48	1.05	-1.57	5448.37	3.21	2.23	0.86	-1.65	7120.56	3.15	2.15	0.79	-1.65
3668.25	3.45	2.45	0.98	-1.65	5684.59	3.27	2.32	0.92	-1.64	7147.56	3.16	2.14	0.80	-1.65
3878.59	3.35	2.39	0.94	-1.70	5713.45	3.31	2.33	0.94	-1.59	7169.59	3.18	2.16	0.78	-1.65
3881.55	3.30	2.38	0.94	-1.70	5773.00	3.33	2.36	0.94	-1.58	7182.54	3.16	2.16	0.80	-1.65
3890.61	3.37	2.41	0.96	-1.64	5775.00	3.32	2.36	0.96	-1.62	7191.57	3.15	2.16	0.79	-1.67
3918.52	3.36	2.43	0.98	-1.69	5801.00	3.32	2.35	0.93	-1.60	7204.48	3.14	2.16	0.79	-1.66
3949.41	3.31	2.39	0.94	-1.74	5846.00	3.32	2.34	0.94	-1.59	7235.46	3.14	2.17	0.80	-1.61
3999.30	3.42	2.45	0.99	-1.62	5874.00	3.35	2.36	0.96	-1.56	7242.39	3.20	2.19	0.81	-1.61
3999.31	3.41	2.44	1.00		5893.00	3.31	2.34	0.93	-1.63	7260.38	3.22	2.21	0.84	-1.61
4002.26	3.42	2.45	1.02	-1.58	6033.58	3.30	2.35	0.94	-1.62	7329.28	3.26	2.24	0.84	-1.58
4240.58	3.36	2.40	0.96	-1.65	6041.59	3.31	2.39	0.98	-1.56	7367.20				-1.58
4251.58	3.38	2.40	0.98	-1.65	6074.54	3.29	2.35	0.93	-1.63	7532.55	3.15	2.19	0.80	-1.67
4282.52	3.41	2.45	1.01	-1.59	6082.56	3.27	2.35	0.93	-1.66	7580.48	3.17	2.23	0.84	-1.63
4290.50	3.40	2.48	1.02	-1.65	6108.45	3.27	2.35	0.94	-1.65	7607.46	3.18	2.20	0.82	-1.64
4308.44	3.40	2.43	1.00	-1.66	6110.41	3.27	2.34	0.92	-1.65	7629.34	3.14	2.20	0.78	-1.70
4320.28	3.40	2.44	0.99	-1.65	6130.50	3.33	2.34	0.92	-1.60	7668.26	3.16	2.17	0.80	-1.63
4328.38	3.42	2.45	0.99	-1.63	6131.42	3.33	2.37	0.95	-1.61	7687.24	3.14	2.14	0.77	-1.66
4353.29	3.44	2.43	0.97	-1.61	6152.33	3.34	2.34	0.91	-1.62	7889.60	3.07	2.08	0.74	-1.66
4360.24	3.41	2.43	0.97	-1.65	6181.32	3.34	2.33	0.90	-1.56	7895.62	3.04	2.08	0.74	-1.72
4364.25	3.40	2.45	0.96	-1.67	6197.34	3.33	2.33	0.91	-1.59	7907.56	3.05	2.09	0.75	-1.70
4381.25	3.39	2.42	0.96	-1.68	6218.23	3.35	2.30	0.89	-1.56	7926.57	3.05	2.10	0.76	-1.69
4591.58	3.31	2.27	0.84	-1.75	6223.29	3.35	2.30	0.88	-1.60	7987.40	3.04	2.07	0.72	-1.69
4609.58	3.30	2.28	0.82	-1.78	6264.22	3.29	2.28	0.87	-1.62	8026.26	3.05	2.08	0.74	-1.65
4620.59	3.28	2.25	0.82	-1.74	6394.56	3.26	2.26	0.83	-1.73	8068.25	3.05	2.03	0.68	-1.66
4622.50	3.27	2.23	0.80	-1.75	6438.57	3.24	2.23	0.82	-1.71	8213.58	2.95	1.95	0.63	-1.75
4625.52	3.23	2.23	0.83	-1.77	6454.55	3.24	2.21	0.79	-1.72	8281.53	3.01	2.04	0.71	-1.69
4631.51	3.21	2.20	0.80	-1.75	6462.50	3.13	2.14	0.71		8297.43	3.00	2.03	0.69	-1.71
4639.48	3.25	2.25	0.84	-1.72	6479.50	3.31	2.26		-1.69	8320.62	3.01	1.99	0.65	-1.72
4644.54	3.23	2.23	0.80	-1.86	6483.48	3.16	2.14	0.74	-1.76	8389.31	3.01	1.99	0.65	-1.69
4646.47	3.28	2.25	0.79	-1.75	6486.33	3.22	2.17	0.76	-1.69	8427.26	3.03	1.99	0.65	-1.69
4648.50	3.26	2.22			6495.45	3.20	2.19	0.78	-1.75	8452.22	2.99	1.97	0.63	-1.74
4668.45	3.23	2.18	0.76	-1.77	6498.46	3.17	2.16	0.75	-1.76	8630.50	2.95	1.92	0.58	-1.74
4672.45	3.21	2.17	0.73	-1.80	6503.42	3.20	2.16	0.75	-1.70	8666.53	2.93	1.91	0.58	-1.73
4681.30	3.23	2.16	0.74	-1.79	6507.38	3.19	2.15	0.75	-1.73	8721.33	2.93	1.89	0.58	-1.73
4685.37	3.21	2.19	0.79	-1.75	6536.35	3.13	2.11	0.72	-1.79	8761.24	2.87	1.82	0.56	-1.75
4720.23	3.10	2.03	0.66	-1.81	6548.32	3.13	2.10	0.70	-1.79	8783.26	2.96	1.89	0.67	-1.61
4907.59	3.02	2.01	0.72	-1.74	6589.23	3.10	2.09	0.70	-1.74	8960.57	2.97	1.93	0.63	-1.68
4928.58	3.11	2.10	0.80	-1.65	6627.22	3.12	2.08	0.70	-1.70	8986.58	2.96	1.92	0.64	-1.67
4949.58	3.08	2.08	0.75	-1.73	6775.57	3.15	2.08	0.81	-1.51	8988.59	2.97	1.94	0.64	-1.70
										8990.58	2.97	1.94	0.65	-1.69
										8991.62	2.96	1.94	0.64	-1.71
										8992.60	2.90	1.91	0.63	-1.74
										9106.30	2.94	1.93	0.64	-1.68
										9142.29	2.93	1.93	0.65	-1.65
										9300.60	2.86	1.90	0.63	-1.67

Sutherland, with a 36-arcsec aperture. They are accurate to better than  $\pm 0.03$  mag at *JHK*, and better than  $\pm 0.05$  mag at *L*. Fig. 1 illustrates the light curves, including some early data reported in Paper I but not included in Table 1 of this paper.

Fig. 2 shows the visual light curve on the same scale as Fig. 1. The data are produced from table 4 of van Genderen et al. (1993), using their equation (2) to approximate the visual magnitude,  $V_1$ , on the Johnson system.

### 3 THE VARIABILITY

Three types of variability are evident in Fig. 1. First, there is an apparently secular increase in brightness. This is most prominent in the *H* photometry, and does not obviously affect the *L* measurements. Secondly, there is a quasi-periodic change on a time-scale of about 5 yr. This variation is present in all the light curves, but its amplitude is largest at *H* ( $\sim 0.4$  mag) and smallest at *L* ( $\sim 0.2$  mag). Thirdly, there

are variations on much shorter time-scales, such as the brightness decreases around JD 244 6700 and 244 7300. All three types of variability are also evident in the visual light curve in Fig. 2.

#### 3.1 The secular changes

##### 3.1.1 A simple model

As has already been stressed, the structure of  $\eta$  Carinae is very complex, and a full model can only be derived from a detailed study of the change with time of this structure over a wide range of wavelengths. Nevertheless, it is possible to draw some general conclusions from integrated photometry, such as that reported here. Extensive earlier studies have shown that four is the minimum number of components required to explain the overall behaviour of this object. These components are (A) a central (hot) high-luminosity source, presumably a massive star, (B) a region of ionized plasma or an extended stellar atmosphere (not necessarily

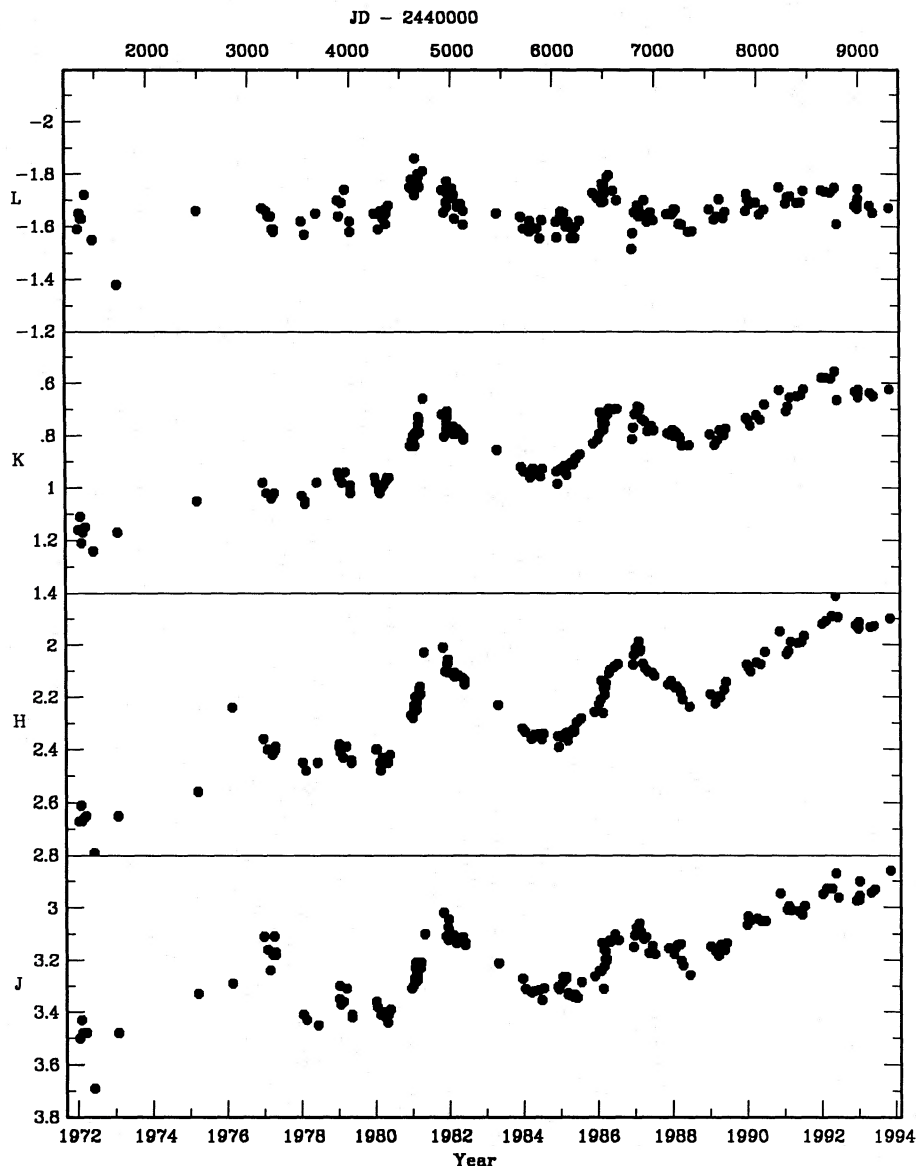


Figure 1. Near-infrared light curves of  $\eta$  Carinae.

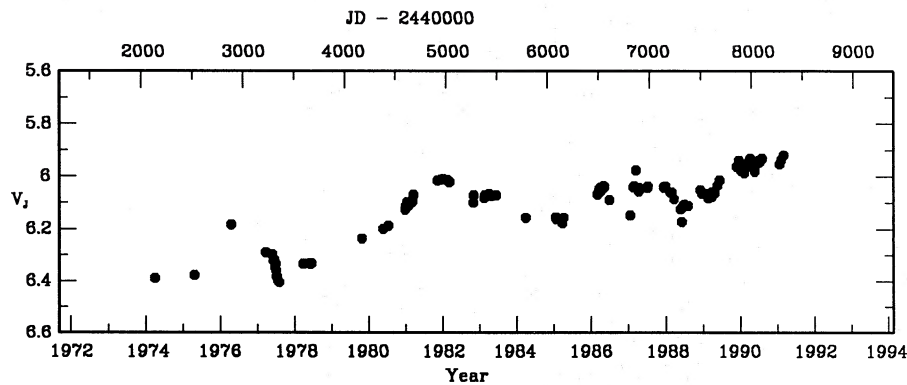


Figure 2. The visual light curve from van Genderen et al. (1993).

spherically symmetric), (C) a (hot) inner dust shell (about 2-arcsec diameter) and (D) an outer (about 15-arcsec diameter) dust shell (the homunculus), which is expanding and was ejected from the central object in the major outburst of 1843. In addition, we shall need to refer to the central few arcsec of the object as seen from the Earth which we refer to as the core (following Hillier & Allen 1992).

Broadly speaking, the main contributions of these components to the observed radiation at different wavelengths are as follows.

(1) Radiation at 5  $\mu$ m, 10  $\mu$ m and longer wavelengths is mainly from the dust in component D (the homunculus). This dust is heated by ultraviolet radiation from component A, which is not seen directly, being hidden from view by an asymmetric absorbing cloud, perhaps component C (e.g. Hillier & Allen 1992).

(2) Around 2  $\mu$ m, the radiation observed is from heated dust in component C, together with a contribution from emission lines and continuum from component B.

(3) The emission lines and continuum observed in the visual region and at shorter wavelengths are primarily produced in component B. The bulk of the radiation from component B is obscured from direct view (probably by component C), and we see this radiation primarily by reflection (scattering) in component D (the homunculus). Some additional radiation, mainly [Fe II] emission lines, is seen more directly towards the central object (i.e. in the core), and some low-excitation emission lines arise from gas mixed with the dust in component D.

(4) The far-ultraviolet radiation from component A provides most of the power for the system.

Item (3) implies a lack of spherical symmetry, and this makes it virtually impossible to construct a meaningful energy budget.

We now consider what the secular variations observed at various wavelengths tell us about the temporal behaviour of these principal components.

### 3.1.2 The visual region

Thackeray (1953) estimated that the visual magnitude of the homunculus was about 6.5, and that of the central core about 8, during 1945/1950. According to van Genderen & Thé (1984), the corresponding data for 1983 are 6.3 and 7 mag.

Thackeray pointed out that, in view of the fact that the visual brightness of the system is dominated by the luminosity of the homunculus, the visual brightening observed in the 1950s must have been primarily due to an increased luminosity of this subsystem. Van Genderen et al. (1994) have further discussed the brightening of the system (homunculus plus core), and have concluded that the visual brightness increased by about 2 mag between 1935 and 1992. This suggests that the brightening of the homunculus noted by Thackeray has continued, since if only the core had varied it would by now totally dominate the visual appearance of the system. However, whilst it seems that there has been a long-term increase in the light scattered from the homunculus, we cannot rule out the possibility that the changes of a few tenths of a magnitude in the visual region over the last 20 yr or so (the only period during which there have been infrared observations) were due primarily to a brightening of the central core.

It must also be remembered that, in view of the peculiar and possibly changing energy distribution of the system and its extended nature, the conversion of the old data, including photographic magnitudes, to a single 'visual' system is subject to considerable uncertainty.

### 3.1.3 The 1.2–3.5 $\mu$ m (JHKL) region

As Fig. 1 shows, there is a secular increase in the flux at *JHK* over the last 22 yr or so. A linear, least-squares fit to the data indicates changes of  $\Delta J \sim 0.6$ ,  $\Delta H \sim 0.8$ ,  $\Delta K \sim 0.6$  and  $\Delta L < 0.1$  mag. Because of the quasi-periodic variations discussed below, it is not possible to say with certainty whether the secular variations take place at a uniform rate or in essentially discontinuous jumps.

### 3.1.4 The 5-, 10- and 100- $\mu$ m region

The data at wavelengths greater than 3.5  $\mu$ m are very sparse. Measurements at these wavelengths are usually made with small apertures in order to minimize thermal noise from the sky. The fact that  $\eta$  Carinae is not a point source makes a comparison of measurements through different, small apertures rather uncertain. Allen (1989) noted that his *M* (4.8- $\mu$ m) measurement in 1985 December was fainter by  $\Delta M = 0.47$  mag than that of Robinson, Hyland & Thomas (1973) in 1971/1972, hinting at a secular decrease at this

wavelength. Four measures in 1986/87 (van Genderen et al. 1994) are similar to that of Allen. However, the 1986 measurement by Russell et al. (1987) is within about 10 per cent of the Robinson et al. values for 1971/1972.

Russell et al. (1987) point out that their 10- $\mu\text{m}$  magnitude in 1986 is fainter by  $\sim 0.3$  mag than that by Robinson et al. (1973) in 1971/72, again hinting at a secular decrease in brightness. There is some evidence that the flux at 100  $\mu\text{m}$  increased between 1977 ( $5200 \pm 1600$  Jy, Harvey, Hoffmann & Campbell 1987) and 1983, when it was measured by the IRAS satellite ( $8200 \pm 1500$  Jy, IRAS Science Team 1988).

### 3.1.5 Models of the secular variability

We now consider the constraints that the observations discussed above place on the model of  $\eta$  Carinae. It is clearly impossible to rule out models in which a number of essentially unrelated phenomena conspire to produce the effects observed. We simply look for a model with the minimum number of postulates.

The bulk of the homunculus is expanding at  $\sim 750$  km  $\text{s}^{-1}$ , and is radiating at a temperature of  $\sim 375$  K. If the ultraviolet (heating) flux from the central object remains constant, we expect the temperature to drop with time due to the expansion. The (tentative) secular decreases in flux at 5 and 10  $\mu\text{m}$ , and the increase at 100  $\mu\text{m}$  can plausibly be attributed to this expansion and temperature drop. Thus, in a simple model involving a single expanding shell, which is assumed to remain optically thick in the ultraviolet and to radiate as a blackbody, one expects over 14 yr a drop in brightness at 4.8  $\mu\text{m}$  of  $\Delta M \sim 0.25$  mag, a practically constant luminosity at 10  $\mu\text{m}$ , and an increase by a factor of 1.2 at 100  $\mu\text{m}$ .

Given the known expansion of the homunculus, it was realized from an early date that a possible reason for the secular increase in visual brightness was a decrease in circumstellar extinction (e.g. Davidson 1971). However, as was made clear in Paper I, the secular increase in the *JHK* flux rules out a simple model of this kind unless the dust produces near-neutral extinction. Our new data clearly strengthen this conclusion. For a standard interstellar reddening law, an increase in brightness of the central core of  $\Delta K \sim 0.4$  mag implies a brightening of the core by  $\Delta V \sim 4.4$  mag and  $\Delta B \sim 5.8$  mag. Depending on the properties of the dust grains, the scattered light from the homunculus may also change but, whether this has increased or decreased in brightness, it is clear that the core has not brightened by  $\sim 4.4$  mag in *V* during the last 20 yr.

In fact, we cannot immediately rule out a dust model with near-neutral extinction. Robinson et al. (1987), in a discussion of the 8–13  $\mu\text{m}$  spectrum of  $\eta$  Carinae, proposed a dust model with an inner hot region (corresponding to our component C) composed mainly of small grains (radius  $\sim 0.2$   $\mu\text{m}$ ), and an outer region (corresponding to the homunculus = component D) composed mainly of large grains (radius  $\sim 2.0$   $\mu\text{m}$ ). These large grains might well produce a reddening law that would explain the observed wavelength dependence of the secular increase. Further work is required to determine whether polarization observations of the homunculus (which have generally been interpreted in terms of small particles) do, in fact, rule out the large-particle hypothesis (see Robinson et al. 1987).

Two alternatives to this large-particle model are the following.

(1) Place the dust responsible for the decreasing extinction in or close to the core and adjust the geometry to get the observed changes in the core and homunculus at various wavelengths.

(2) Attribute the secular brightening not to decreasing extinction, but to a real increase in luminosity of components B and C. This is not a priori improbable, since these components may well be gaining matter as a result of the outbursts of the central object, which are discussed below.

It will be clear that the above two alternative hypotheses, together no doubt with others that may be devised, contain many free parameters and will therefore be more difficult to test than that of large particles in the homunculus. Evidently, if the *JHK* brightening is due to decreasing extinction in the homunculus, the rate of brightening should gradually decrease. The behaviour at visual wavelengths will depend on the relative scattering and absorption efficiencies of the grains. The secular brightening at 2.2  $\mu\text{m}$ , together with the tentative evidence for fading at 5 and 10  $\mu\text{m}$ , suggests that the long-term near-constancy at *L* (3.5  $\mu\text{m}$ ) over the last 20 yr has been a balance between contributions from the hot and the cold dust (components C and D) at this wavelength.

One cannot entirely discard the hypothesis that the secular changes are due to a long-term increase in luminosity of the central engine. The apparent variation at 5  $\mu\text{m}$  and longer wavelengths discussed above does not seem to require such a model, but more frequent and high-accuracy observations at these wavelengths are desirable.

## 3.2 The quasi-periodic changes

### 3.2.1 Fourier analysis

The data from Table 1 were examined for periodicity, after removing the long-term trend using a linear least-squares fit of the form

$$m(t) = c_0 + c_1 t, \quad (1)$$

where  $m(t)$  is the *J*, *H*, *K*, *L* or *V<sub>J</sub>* magnitude at a time  $t = \text{JD} - 244\,0000$ . The coefficients,  $c_0$ ,  $c_1$ , found from the fits are listed in Table 2, with their standard errors in brackets. No significant slope was found for the *L* data over this approximately 18-yr period. The same procedure was followed with the *V<sub>J</sub>* magnitude illustrated in Fig. 2; note, however, that these data cover a shorter time-interval than do the infrared observations, and may therefore show slightly different systematic effects.

The data from which the trend (as specified by equation (1) and Table 2) had been removed were Fourier-trans-

**Table 2.** Coefficients of equation (1).

	$c_0$	$c_1$ (mag day $^{-1}$ )
<i>J</i>	$-149(\pm 9)$	$-0.58(\pm 0.05) \times 10^{-4}$
<i>H</i>	$-139(\pm 12)$	$-0.77(\pm 0.05) \times 10^{-4}$
<i>K</i>	$-185(\pm 13)$	$-0.58(\pm 0.04) \times 10^{-4}$
<i>L</i>	$-8(\pm 7)$	$-0.03(\pm 0.03) \times 10^{-4}$
<i>V<sub>J</sub></i>	$-149(\pm 9)$	$-0.64(\pm 0.04) \times 10^{-4}$

**Table 3.** Frequencies present in the photometry.

	Frequency cycles day <sup>-1</sup> ( $\times 10^4$ )	Amplitude (mag)	Period (day)
J	5.463	0.19	1830
	3.600	0.11	2780
H	5.354	0.24	1870
	2.950	0.08	3390
	10.10	0.10	990
K	5.287	0.17	1890
	2.923	0.07	3420
	10.32	0.07	970
L	5.394	0.10	1850
	11.13	0.06	900
	3.716	0.05	2690
V <sub>J</sub>	2.541	0.14	3940
	32.81	0.07	305
	10.21	0.06	980

formed, and the periodogram was examined. Table 3 lists the three most significant periods found for each colour, and their peak-to-peak amplitudes. A period of 9775 d found in the *J* data is not listed, as it is approximately equal to the total time-span of the data. The nominal standard error on the amplitudes is  $\pm 0.01$  mag. There are, however, systematic deviations of the observations from the fitted curves (see, e.g., Fig. 3, which is discussed below). This is a well-known, but little-mentioned, phenomenon of variable-star light curves. The systematic nature of the deviations implies that the residuals are positively correlated. A consequence of this is that standard errors calculated in the usual way may severely underestimate the true parameter uncertainties. A more comprehensive discussion of this problem is given by Fuller (1976, section 9.7).

A period of between 1830 and 1890 d is found in all of the infrared colours. A second period of between 900 and

990 d, which is probably the first harmonic of the 1830–1890 d period, is found in the *HKL* data and in the independent *V<sub>J</sub>* magnitudes. From this, it is apparent that there are quasi-periodic variations present in the photometry under discussion. It is not clear if they are physically meaningful, or if they might reasonably be expected to persist over a much longer time-interval.

In fact, a reasonable reproduction of the gross variations, including the apparently secular brightness increase, can be achieved by fitting the data with two periods and their first harmonics. Fig. 3 shows the result of fitting the *H* data with a 50 000-d period (and harmonic) to represent the long-term trends, plus an 1850-d period (and harmonic). The rms residual from this fit is 0.035 mag. Again it is not clear that this is telling us anything more than that  $\eta$  Carinae varies on a time-scale of about 5 yr. This is a typical time-scale for LBV outbursts, the causes of which are not yet established, although a number of suggestions have been made (e.g. Stothers & Chin 1983; Lamers 1987; de Koter 1993). It is interesting to note that in  $\eta$  Carinae these variations are more prominent at *H* than at any other wavelength.

It is possible that the 1850-d variation is the consequence of radial pulsation, of the star itself, or of the H II region immediately surrounding the star, or even of the warm inner dust shell. With regard to pulsation of the star itself, the pulsation equation can be expressed as (Cox 1974)

$$P = 2\pi[(3\Gamma - 4)(4/3)\pi G\bar{\rho}]^{-1/2}, \quad (2)$$

where  $G$  is the gravitational constant, and  $\bar{\rho}$  is the mean density of the star. The adiabatic exponent for the gas,  $\Gamma$ , is given by  $\Gamma = \delta \ln P / \delta \ln \rho$ . A normal blue supergiant would pulsate with a rather short fundamental period, of the order of 10 d or possibly less. However,  $\eta$  Carinae is thought to be a very massive star undergoing mass loss. Under these circumstances, radiation pressure will dominate gas pressure and  $\Gamma$  could be very close to 4/3. Thus the pulsation period could be very long, and a value such as 1850 d is plausible. Note also that, if  $\eta$  Carinae is pulsating in this way, we would not expect it to show a stable period. It is obviously not possible to make a quantitative estimate of the pulsation period, or to predict the way the period may change, without a detailed model of the star.

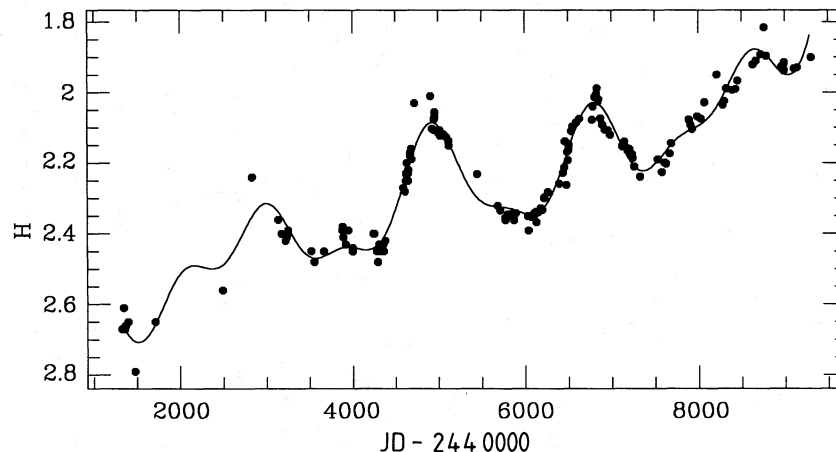


**Figure 3.** The *H* (1.65- $\mu$ m) light curve, fitted with a double-period, second-order sine curve. The periods used were 50 000 d (to represent the secular changes) and 1900 d.

A more detailed discussion of this and other aspects of pulsation in LBVs was provided by Stothers & Chin (1983). Note, however, that Appenzeller (1986) concluded that stars pulsating in this way would not deviate substantially from the equilibrium models, and that the main effect of the pulsation will be an increased mass loss. In addition, the work of Stothers (1992) indicates that  $\eta$  Carinae, as an evolved rather than a main-sequence star, would be stable against such pulsation.

### 3.2.2 Randomly driven cycles

An alternative to the interpretation of the observations as deterministic (i.e. completely predictable) cycles with superimposed noise is a model of randomly driven cycles. Such a model has, for example, been fitted to annual sunspot numbers (Phadke & Wu 1974). The model for the observed magnitudes  $m(t)$  is

$$D^p m(t) + a_{p-1} D^{p-1} m(t) + \dots + a_1 D m(t) + a_0 m(t) = \epsilon(t), \quad (3)$$

where the  $a_i$  are constant,  $D = d/dt$  is the differential operator, and  $\epsilon(t)$  is a randomly fluctuating driving 'force' with a zero mean and a standard deviation  $\sigma_\epsilon$ . The source of the variations  $\epsilon(t)$  could be, for example, random brightening and fading of the luminosity, or random transparency changes in the circumstellar material. Jones (1981) describes how such models can be fitted to irregularly spaced observations, such as those in Table 1. The model parameters are estimated by a maximum-likelihood procedure, the likelihood being evaluated using Kalman filtering methods (Kalman & Bucy 1961). Allowance may be made for observational error (with standard deviation  $\sigma_0$ ).

**Table 4.** Results of fitting equation (3) to the photometry.

	$a_0$	$a_1$	$\sigma_\epsilon$	$\sigma_0$	$P$ (day)
J	$3.1 \cdot 10^{-5}$	$9.8 \cdot 10^{-2}$	$7.4 \cdot 10^{-5}$	$2.8 \cdot 10^{-2}$	2385
	$1.7 \cdot 10^{-3}$		$5.5 \cdot 10^{-3}$	$2.4 \cdot 10^{-2}$	588
H	$2.6 \cdot 10^{-4}$	$5.3 \cdot 10^{-3}$	$5.4 \cdot 10^{-4}$	$2.2 \cdot 10^{-2}$	1455
	$1.7 \cdot 10^{-3}$		$5.7 \cdot 10^{-3}$	$1.6 \cdot 10^{-2}$	588
K	$2.1 \cdot 10^{-5}$	$4.2 \cdot 10^{-3}$	$2.8 \cdot 10^{-5}$	$2.4 \cdot 10^{-2}$	1524
	$2.5 \cdot 10^{-3}$		$5.0 \cdot 10^{-3}$	$1.5 \cdot 10^{-2}$	400
L	$5.2 \cdot 10^{-3}$		$5.0 \cdot 10^{-3}$	$2.9 \cdot 10^{-2}$	192
$V_J$	$3.2 \cdot 10^{-3}$		$5.7 \cdot 10^{-3}$	$1.9 \cdot 10^{-2}$	312

For second-order equations (i.e. only  $a_1, a_0 \neq 0$ ), the natural period of the system is  $P = 2\pi/\sqrt{a_0 - 0.25a_1^2}$ . For first-order equations, the decay time is  $P = 1/a_0$ . Table 4 shows the results for the infrared data from Table 1, after correcting for the secular variations using equation (1) with the coefficients of Table 2. The choice between different orders of equation (3) is made on the basis of the Akaike information criterion; this is essentially a sum of residual squares with a penalty for the number of parameters fitted. For  $J$  and  $H$ , second-order solutions are preferred; for  $K$  and  $L$ , first-order solutions are preferred. No oscillatory second-order solution could be found for  $L$  or  $V_J$ . The units of the quantities listed in Table 4 are as follows (where time,  $t$ , is in d): for second-order solutions,  $[a_1] = t^{-1}$ ,  $[a_0] = t^{-2}$ ,  $[\sigma_\epsilon] = \text{mag} \times t^{-2}$ ; for first-order solutions,  $[a_0] = t^{-1}$ ,  $[\sigma_\epsilon] = \text{mag} \times t^{-1}$ . Fig. 4 shows the filtered  $H$  observations. Approximate confidence bounds for the estimated parameters may be found by using asymptotic properties of the maximum-likelihood estimates. This is far from trivial, and work on it is in progress (Koen 1993, in preparation).

The results of Table 4 may be interpreted as follows: the variations in  $L$  and  $V_J$  are not sufficiently close to strict periodicity to allow modelling as random cycles (the same point is evident in the small amplitudes of the periodogram peaks for these observations). It is clearly attractive to interpret all the observations in a single framework; this is possible if one adopts the simple model  $Dm(t) + a_0 m(t) = \epsilon(t)$  for all of the data. Fig. 5 shows the results of two independent simulations of the  $H$  magnitude using this expression and the first-order parameters listed in Table 4. The implication of this particular model is that there is no true periodicity in the data. The apparent cyclicity is caused solely by the relatively long memory structure of the data implied by the values of  $P$  ( $P = 1/a_0$ ) in Table 4. A similar phenomenon has been pointed out in other astronomical contexts by Terrell & Olsen (1970) and Terrell (1972). Although the simulations in Fig. 5 provide a good representation of the apparent 5-yr cycles seen in the data (Fig. 4), they also tend to show more prominent shorter period variations (200 to 400 d) than are evident in the data.

The values of the 'period' ( $P$ ) in Table 4 hold certain implications for the structure of  $\eta$  Carinae: the 'memory' of the  $J$  and  $H$  response to source variations is long, the  $L$  coherence short, and the  $K$  and  $V_J$  intermediate. Various interpretations of these results are possible, but somewhat outside the scope of this paper.

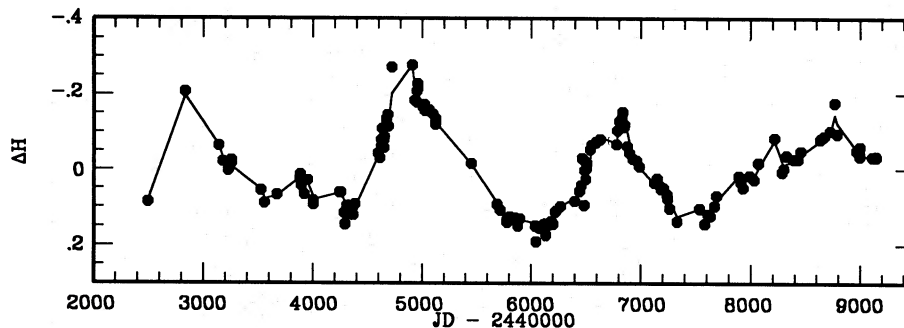


**Figure 4.** The  $H$  light curve, after the trend has been removed as described in Section 3.2.1. The solid line represents the filtered  $H$  observations, i.e. the estimated 'signal' underlying the observational 'noise'.

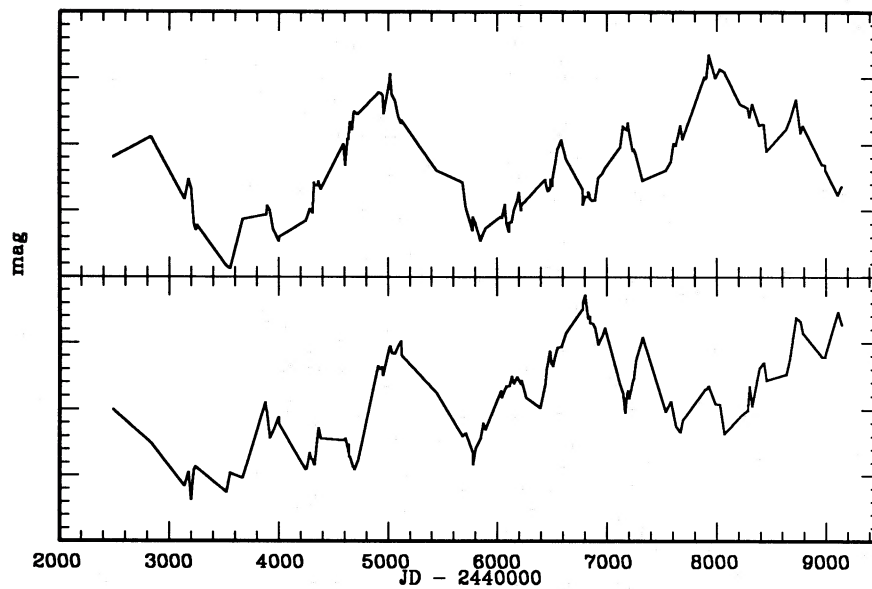


Figure 5. Model simulations, as discussed in Section 3.2.2.

### 3.2.3 Other aspects of the quasi-periodic changes

Paper I and Zanella et al. (1984) discussed spectral changes associated with the 1981/82 brightness peak. They found that the normally prominent high-excitation lines, in particular [Ne III], [Fe III] and He I, were weak when  $\eta$  Carinae was bright. A similar weakening has been noted at various times in the past, specifically in 1948 (Gaviola 1953; Viotti 1968) and in 1965 (Rodgers & Searle 1967; Thackeray 1967).

These variations have been attributed to changes in temperature of the central star (Paper I; van Genderen & Thé 1984) or to the ejection of a shell and subsequent condensation of dust in the ejecta (Zanella et al. 1984). It is not clear that these explanations are mutually exclusive. A change in temperature of the central source and the ejection of a shell could both be consequences of radial pulsation which was discussed above. The more general and probably (though not necessarily) related problem of variability in LBVs has been discussed by, e.g., Appenzeller (1986), Lamers (1987), Leitherer et al. (1989) and de Koter (1993).

An alternative mechanism for the variability is the dynamical instability noted by Stothers & Chin (1993) to be a consequence of the high iron opacity in the outer envelopes of very massive stars. Calculations performed by Stothers & Chin suggested that slow relaxation oscillations develop, which show rapidly growing amplitude and lengthening period. In  $\eta$  Carinae we may see the lengthening period. In fact, if the 1110-d variations, noted by Feinstein & Marraco (1974) in optical photometry pre-dating that under discussion, were real (their data are not convincing on this point), then they might have been the first indication of the variability reported here. The amplitude of the variations in  $\eta$  Carinae is not obviously growing (see Fig. 4), although it is difficult to separate precisely the quasi-periodic changes from the secular ones discussed above. Stothers & Chin further suggest that the blue and visual variations will be large, while the bolometric changes will be small. Dust

particles absorb ultraviolet and blue radiation much more efficiently than they do longer wavelengths. The behaviour of the hot dust should therefore provide a good indication of variations in the blue luminosity of the underlying star. Clearly, data over a longer time-interval are required before any firm conclusions can be drawn on the cause of the variation.

### 3.3 Short-time-scale variations

There are features in Fig. 1 which indicate that variations occur on time-scales of 100 d or less. Where the temporal coverage is good enough, these short-time-scale variations appear in the completely independent visual light curve (Fig. 2) as well as the infrared data. Note, in particular, the changes around JD 2446700 and 2447370. van Genderen et al. (1994) have suggested that some of these events are the consequences of eclipses. The evidence presented in support of this suggestion is not particularly convincing, but more work is clearly necessary before a realistic interpretation can be offered.

## 4 CONCLUSION

$\eta$  Carinae has been brightening slowly over the last 20 yr at wavelengths between 1 and 2.5  $\mu\text{m}$ . A similar change has been noted at visual wavelengths. There is some indication that it is becoming fainter at mid-infrared wavelengths ( $\sim 4$  to 14  $\mu\text{m}$ ). If these changes are due to the gradual thinning of dust obscuration in the homunculus, then the dust must be predominantly in the form of large grains.

The near-infrared data show quasi-periodic variations on a time-scale of 5 yr. These variations may be of the same nature as those of comparable time-scale which are a well-established feature of LBVs. Pulsation is one of several possible causes of this behaviour.

There are also clear indications of changes on a significantly shorter time-scale, for which no satisfactory explanation is yet available.

## ACKNOWLEDGMENTS

We are grateful to the following people for making some of the infrared observations: F. Marang, R. M. Catchpole, J. Spencer Jones, C. D. Laney and I. S. Glass.

## REFERENCES

- Allen D. A., 1989, *MNRAS*, 241, 195  
 Appenzeller I., 1986, in De Loore C. W. H. et al., eds, *Proc. IAU Symp. 116, Luminous Stars and Associations in Galaxies*. Reidel, Dordrecht, p. 139  
 Bath G. T., 1979, *Nat*, 282, 274  
 Borgwald J. M., Friedlander M. W., 1993, *ApJ*, 408, 230  
 Carter B. S., 1990, *MNRAS*, 242, 1  
 Cox J. P., 1974, *Rep. Prog. Phys.*, 37, 563  
 Davidson K., 1971, *MNRAS*, 154, 415  
 de Koter A., 1993, PhD thesis, Univ. Utrecht  
 de Vaucouleurs G., Eggen O. J., 1952, *PASP*, 64, 185  
 Feinstein A., Marraco H. G., 1974, *A&A*, 30, 271  
 Fuller W. A., 1976, *Introduction to Statistical Time Series*. Wiley, New York  
 Gallagher J. S., 1989, in Davidson K. et al., eds, *Physics of Luminous Blue Variables*. Kluwer, Dordrecht, p. 185  
 Gaviola E., 1953, *ApJ*, 118, 234  
 Gratton L., 1963, in Gratton L., ed., *Star Evolution*. Academic Press, New York, p. 297  
 Harvey P. M., Hoffmann W. F., Campbell M. F., 1978, *A&A*, 70, 165  
 Hester J. J., Light R. M., Westphal J. A., Currie D. G., Groth E. J., Holtzman J. A., Lauer T. R., O'Neil E. J., 1991, *AJ*, 102, 654  
 Hillier D. J., Allen D. A., 1992, *A&A*, 262, 153  
 Hyland A. R., Robinson G., Mitchell R. M., Thomas J. A., Becklin E. E., 1979, *ApJ*, 233, 145  
 Innes R. T. A., 1903, *Cape Annals* 9, 75B  
 IRAS Science Team, 1988, *IRAS Point Source Catalog*  
 Jones R. H., 1981, in Findley D. F., ed., *Applied Time Series Analysis II*. Academic Press, London  
 Kalman R. E., Bucy R. S., 1961, *J. Basic Engineering: Trans. ASME D*, 83, 95  
 Lamers H. J. G. L. M., 1987, in Lamers H. J. G. L. M., de Loore C. W. H., eds, *Instabilities in Luminous Early Type Stars*. Kluwer, Dordrecht, p. 99  
 Leitherer C., Schmutz W., Abbot D. C., Hamann W.-R., Wessolowski U., 1989, *ApJ*, 346, 919  
 Maeder A., 1990, in Willson L. A., Stalio R., eds, *Angular Momentum and Mass Loss for Hot Stars*. Kluwer, Dordrecht, p. 33  
 Neugebauer G., Westphal J. A., 1968, *ApJ*, 152, L89  
 O'Connell (SJ) D. J. K., 1956, *Vistas Astron.*, 2, 1165  
 Phadke M. S., Wu S. M., 1974, *J. Am. Stat. Assoc.*, 69, 325  
 Robinson G., Hyland A. R., Thomas J. A., 1973, *MNRAS*, 161, 281  
 Robinson G., Mitchell R. M., Aitken D. K., Briggs G. P., Roche P. F., 1987, *MNRAS*, 227, 535  
 Rodgers A. W., Searle L., 1967, *MNRAS*, 135, 99  
 Russell R. W., Lynch D. K., Hackwell J. A., Rudy R. J., Rossano G. S., Castelaz M. W., 1987, *ApJ*, 321, 937  
 Stothers R. B., 1992, *ApJ*, 392, 706  
 Stothers R. B., Chin C.-W., 1983, *ApJ*, 264, 583  
 Stothers R. B., Chin C.-W., 1993, *ApJ*, 408, L85  
 Terrell N. J., 1972, *ApJ*, 174, L35  
 Terrell N. J., Olsen K. H., 1970, *ApJ*, 161, 399  
 Thackeray A. D., 1953, *MNRAS*, 113, 237  
 Thackeray A. D., 1967, *MNRAS*, 135, 51  
 van Genderen A. M., Thé P. S., 1984, *Space Sci. Rev.*, 39, 317  
 van Genderen A. M., de Groot M. J. H., Thé P. S., 1994, *A&A*, 283, 89  
 Viotti R., 1968, *Mem. Soc. Astron. Ital.*, 39, 105  
 Westphal J. A., Neugebauer G., 1969, *ApJ*, 156, L45  
 Whitelock P. A., Feast M. W., Carter B. S., Roberts G., Glass I. S., 1983, *MNRAS*, 203, 385 (Paper I)  
 Zanella R., Wolf B., Stahl O., 1984, *A&A*, 137, 79